# Local Structure of Phosphate/Amine Polyion Complexes in Phospholipid/Polypeptide Mixtures by Solid State NMR and ab Initio Chemical Shielding Calculation

**Naoki Asakawa,* Daisuke Sato, Minoru Sakurai, and Yoshio Inoue**

*Department of Biomolecular Engineering, Graduate School of Bioscience and Biotechnology, Tokyo Institute of Technology, 4259 Nagatsuta-cho, Midori-ku, Yokohama, 226-8501 Japan*

*Received: June 2, 1999*

Local structure of phospholipid/amine polyion complexes in lyophilized powders of dipalmitoylphosphatidic acid(DPPA)/poly-L-lysine(pLYS) and DPPA/poly-L-arginine(pARG) is investigated by solid-state nuclear magnetic resonance spectroscopy. The intermolecular interactions in the polyion complexes were detected by $^{31}P-^{1}H$ heteronuclear shift correlation (HETCOR). The complete information about the $^{31}P$ chemical shift tensor (CST), principal values of CST and the mutual orientation of CST with respect to a molecular fixed frame, for methylguanidinium dihydrogenorthophosphate ($MGD/H_2PO_4$), which is thought of as a model compound for DPPA/pARG, was determined by both cross-polarization and magic-angle sample spinning (CPMAS) and spin−echo separated local field (SLF) measurements under the magic-angle sample spinning (MAS). From the ab initio $^{31}P$ chemical shielding calculation, the behavior of the principal components of $^{31}P$ chemical shield tensor in the phosphate group in DPPA is found to be dominated by a change in the electronic state in association with phosphate/amine complexation, rather than by a change in a bond angle of nonprotonated $\angle O^{(3)}-P-O^{(4)}$ which was previously deduced in several phosphate compounds.

## I. Introduction

Phosphate/amine complexes can be seen in various biochemical systems, such as signal transductions by protein kinases,[1] nucleoprotein complexes, such as chromatin in eukaruotic genome DNA,[2] charge-transfer complexes in supermolecular chemistry,[3] and so on. Phospholipid/polypeptide complexes form one such system and are of particular interest because complexation of phospholipids with polypeptides often brings about unique thermotropic and/or structural properties into phospholipids. Indeed, some membrane proteins require specific phospholipids to activate themselves.[4−6]

A complex of an acidic phospholipid with a basic polypeptide is one of typical polyion complexes, which can provide phosphate/amine complexes with high density. Poly(L-lysine)-(pLYS) and poly(L-argine)(pARG) are representative basic polypeptides, and each amino acid residue of the polypeptides has a positive charge in the side chain at physiological pH. Therefore, the polypeptides are expected to electrostatically bind to negatively charged acidic phospholipids.

So far, it has gradually been understood that such a binding leads to a change in the thermotropic property of the membrane.[7] According to Ohki et al., additions of pLYS and pARG to dipalmitoylphosphatidic acid (DPPA) cause the phase transition temperature from gel ($L'_\beta$ phase) to liquid crystal ($L_\alpha$) to move to about 9 °C higher and about 18 °C lower, respectively, than the transition temperature (ca. 50 °C) of DPPA without these polypeptides. Here, we must note that the transition temperature would vary with depending upon amount and molecular weight of polypeptide, and pH.[8] The thermotropic behavior of the pLYS/DPPA complex has been also interpreted by X-ray diffraction, and it has been concluded that the behavior could be attributed to the fact that pLYS adopts a $\beta$-sheet conformation on the surface of the DPPA bilayers and strengthens the packing structure of the membrane.[9] Any X-ray crystallographic studies for pARG/DPPA complex are not available at the moment because of the highly disordered system.

Solid-state NMR spectroscopy has been thought of as one of powerful methods for analyses of structure and dynamics of biological membranes. Since chemical shift analysis is straightforward to perform, it has possibility to be a complemental methodology for structural study of molecules with other methods such as detection of magnetic dipole coupling if structure−chemical shift (S/C) correlation is established.[10−12] From this viewpoint, we have been investigating the correlation between $^{31}P$ chemical shift tensor (CST) and molecular structure of phospholipids.[13]

In this article, we will attempt to detect the intermolecular interactions in lyophilized powders of the pLYS/DPPA and pARG/DPPA complexes by solid-state $^{1}H-^{31}P$ heteronuclear correlation NMR spectroscopy (HETCOR). Since CSTs of nuclei are thought to be highly relevant to its electronic structure, thus one often seeks to obtain the infomation about principal values of CST. Further, the information about the orientation of CST is of great importance as well as its principal values, because the investigation into the relevance between a principal axis system (PAS) of CST and molecular fixed frame (MFF) is desired. For a polycrystalline sample of methylguanidinium dihydrogenorthophosphate ($MGD/H_2PO_4$), which is thought of as a model compound for local structure of DPPA/pARG, we will extract the complete information about the $^{31}P$ chemical shielding tensor, i.e., three principal components of the CST and relative orientation of its principal axes with respect to the molecular fixed frame for a phosphate group in polycrystalline powder, by using both a conventional cross-polarization[14] and magic-angle sample spining (CPMAS)[15,16] and a spinning sideband (SSB) enhanced version of separated local field measurement. By comparing the experimental CST and ab initio

* To whom correspondence should be addressed.

10.1021/jp9917695 CCC: $19.00 
Published on Web 03/08/2000

GIAO chemical shielding calculation, behaviors of $^{31}P$ chemical shielding tensor for the phosphate group in the two polyion complexes will be investigated.

## II. Materials

**Preparation of DPPA, DPPA/pLYS, and DPPA/pARG.** Dipalmitoylphosphatidic acid (DPPA) sodium salt, poly(L-lysine)·HCl ($M_w$ = 30000−70000), and poly(L-arginine)·HCl ($M_w$ = 15000−70000) were purchased from SIGMA Chemical Co. (St. Louis, MO). All the materials were used without further purification. 2-[4-(2-Hydroxyethyl)-1-piperazinyl]ethanesulfonic acid (HEPES) was purchased from NACALAI TESQUE, INC. (Kyoto, Japan). All the samples used in this article were prepared by the following procedures.

DPPA dispersions were dissolved in 50 mM HEPES (pH 7.5) buffer solution with 23.6 mM NaOH and 76.4 mM NaCl so that the lipid concentration should be 2% (w/w). After being incubated at 80 °C for 2 h, the dispersion was sonicated for 1 min by an ultrasonic disruptor (UR-200P, TOMY SEIKO Co., Tokyo, Japan) and was then incubated at 80 °C for 5 min and was sonicated again for 10 min in order to form small unilamellar vesicle (SUV). The dispersions were mixed with pLYS solution of which molar ratio of the amino acid monomer unit/DPPA should be 1.25:1 (mol/mol). Prior to the mixing, the polypeptide was dissolved in the same amount of the HEPES buffer used above. A large quantity of precipitate was obtained by three heating−cooling cycles for the mixed dispersion (heating to 90 °C, cooling to room temperature). The precipitate of the DPPA/pLYS complex was collected by centrifugation at 9000*g* for 15 min. The precipitate collected was stored at 4 °C for 4 days and then lyophilized. The same protocol was employed for the preparation of pARG/DPPA.

The DPPA and DPPA/HEPES samples for the controlled experiments were prepared by the followings. A desired amount of DPPA was dispersed in water or HEPES buffer so that the lipid concentration should be 1% (w/w). The dispersions were incubated at 80 °C for 2 h and then cooled to room temperature. The samples obtained were stored at 4 °C for 4 days and then lyophilized.

**Preparation of MGD/$H_2PO_4$.** A polycrystalline sample of methylguanidinium dihydrogenorthophosphate for separated local field measurements were prepared by the same procedure by Cotton et al.[17]

## III. Experimental and Theoretical Section

**NMR Measurements.** All the experiments were performed on a Varian Unity400 (9.4 Tesla) or a modified JEOL GSX270 (6.34 Tesla) FT NMR spectrometer equipped with the double resonance tunable MAS probe. The radio-frequency field intensities for the $^1H$ and $^{31}P$ channels were set at 50 kHz. A contact time for the cross-polarization was 2.0 ms. The recycle delay for all the experiments was 5 s. The MAS speed was monitored and controlled by a personal computer with optical fibers. Principal components of chemical shift tensors were determined from spinning sideband (SSB) intensities by a method by Fenzke et al.,[18] which is a modified version of Herzfeld−Berger analysis.[19]

**$^1H-^{31}P$ Heteronuclear Shift Correlation (HETCOR) Measurements.** $^1H-^{31}P$ HETCOR measurements were performed with using a method described by Burum and Bielecki,[20] in order to investigate local structure round the phosphate groups of DPPA/pLYS and DPPA/pARG. The pulse sequence and the phase cycling were shown in Figure 1a. After a preparation pulse of proton magnetization, the BLEW-12 and BB-12 multipulses for the $^1H$ and $^{31}P$ channels were applied to reduce both $^1H-^1H$ and $^1H-^{31}P$ dipolar interactions and to make the Hamiltonian during $t_1$-evolution dependent solely on the $^1H$ chemical shift. Sixteen $t_1$ values were collected with an increment of 120 $\mu$s. Before the mixing period, $\Theta$ ($90°_x$) and $\Phi$ ($63°_{-y}$) pulses were applied to align the effective field of proton generated by BLEW-12 to the *z*-axis. The cross-polarization was carried out by WIM-24 pulse sequence which reduces spin diffusion processes by homonuclear dipolar couplings, enabling us to selectively monitor proton magnetizations proximate to the phosphorus nucleus. During the acquisition period ($t_2$), the CW proton decoupling was carried out. The number of scans was 2048. The MAS speed was set at 4.170 kHz.

**$^{31}P$ Separated Local Field (SLF) Measurements.** To obtain the information about relative orientation of $^{31}P$ CST of methylguanidinium dihydrogenorthophosphate (MGD/$H_2PO_4$) with respect to the molecular fixed frame, the SSB enhanced spin−echo SLF measurements[21] were performed. The pulse sequence is drawn in Figure 1b. Although the pulse sequence does not completely separate the P−H heteronuclear dipolar coupling from the $^{31}P$ chemical shift, we employed the method because the spinning sideband manifold in the $\omega_1$-dimension is thought to be sensitive to the mutual orientation between the chemical shift and the P−H dipolar tensors. We employed a simple pulse sequence, the semi-windowless WHH-4,[22] for decoupling of proton homonuclear dipolar interaction, which would be relatively weak in a head-group of phospholipids. The spectral width in $\omega_1$-dimension was set as 13020 Hz by using semi-windowless WHH-4 with a cycle of 38.4 $\mu$s. The MAS speed was set at 2.888 kHz. Optimization of WHH-4 was carried out with the procedure described by Drobny et al.,[23] and the pulse widths and phases were calibrated by using the method by Gerstein.[24]

**Spectrum Simulation.** NMR spectral simulation programs for Herzfeld−Berger analysis and the spin−echo SLF measurements based on the multiple time-step method were written in C language and were performed on a IBM-AT compatible personal computer. Powder averagings were performed with random orientations with respect to the external magnetic field.

**Chemical Shielding Calculation.** $^{31}P$ chemical shielding tensor calculations of $H_2PO_4^-$ (**I**), methylphosphate monohydrogen [$H(CH_3)PO_4$] (**II**), methylammonium/phosphate complex (**III**), and guanidine/phosphate complex (**IV**) were calculated by an ab initio coupled Hartree−Fock (CHF) method with gauge invariant atomic orbitals (GIAO). Figure 2 depicts the molecules **I**−**IV**. The molecular structures for the above four model compounds were optimized with the 6-31G(p,d) basis set, and the GIAO−CHF calculations were carried out with 6-31G(d,p) or 6-311++G(p,d) basis set. All the ab initio chemical shielding calculations were performed with Gaussian 94 program package (Gaussian, Inc., Pittsburgh, PA) run on a Cray C916/12256 super computer at the Computer Center, Tokyo Institute of Technology.

## IV. Results and Discussion

**Intermolecular Interaction in Phosphate/amine Complexes Detected by $^1H-^{31}P$ HETCOR Measurements.** We investigate the local structure of the polyion complexes by $^1H-^{31}P$ HETCOR measurements. Figure 3 shows the $^1H-^{31}P$ HETCOR spectra for DPPA, DPPA/pLYS, and DPPA/pARG, respectively. The contours of the two-dimensional spectra with $^1H$ projections were shown only for the region of $^{31}P$ isotropic chemical shift. As is described in the Experimental and Theoretical Section, we can selectively monitor proton signals which are located in

## FIGURES

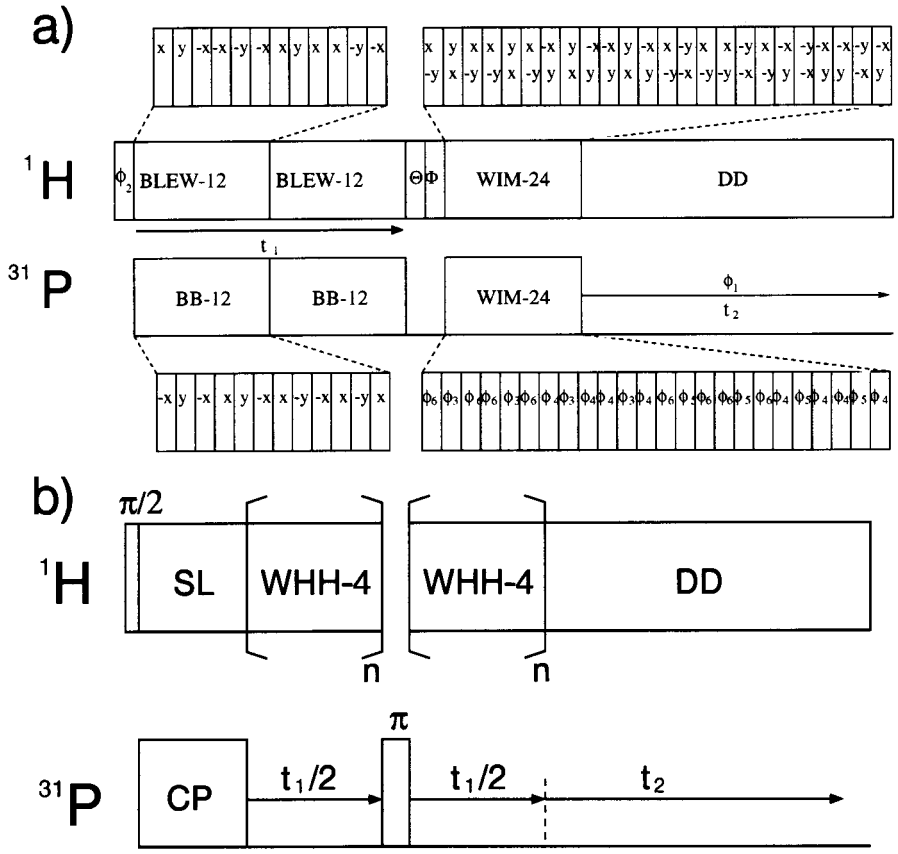


**Figure 1.** . Pulse sequences for $^{31}$P−$^{1}$H heteronuclear correlation (HETCOR) NMR (a) and spin−echo separated local field (SLF) measurements (b) in the solid state. The phases for HETCOR are $\phi_1 = (x, -x, -y, y, -x, x, y, -y)$. $\phi_2 = (x, -x, x, -x, x, -x, x, -x)$. $\phi_3 = (-y, -y, -x, -x, y, y, x, x)$. $\phi_4 = (-x, -x, y, y, x, x, -y, -y)$, $\phi_5 = (y, y, x, x, -y, -y, -x, -x)$, $\phi_6 = (x, x, -y, -y, -x, -x, y, y)$.

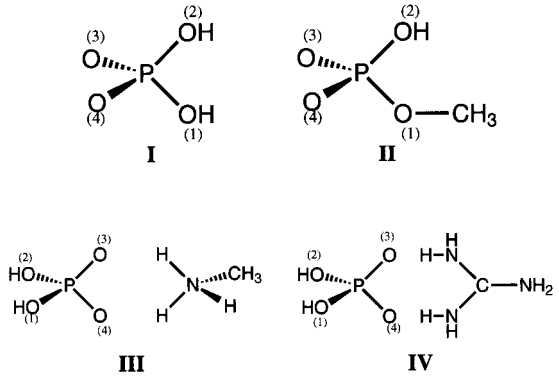


**Figure 2.** Chemical structure of model molecules used in GIAO chemical shielding calculations: $H_2PO_4^-$ (**I**), monohydrogen methylphosphate (**II**), methylammonium/phosphate complex (**III**), and guanidine/phosphate complex (**IV**).

the proximity of the phosphorus nucleus by using the WIM-24 cross-polarization process. We obtained the $^1$H spectra with rather broad signals, which feature has also been seen in the $^1$H−$^{31}$P HETCOR spectra of several phosphate compounds obtained by Santos et al.[25] Signal assignments were performed by using $^1$H chemical shift values of phospholipids intensively investigated in solution NMR and the result by Santos et al.[25] From Figure 3a), the most intensive signal appeared at ∼10 ppm, which can be assigned to the phosphate proton. This proton is the nearest neighbor of the phosphorus atom ($R_{P-H} \approx 2.4$ Å). A signal at ∼6 ppm can be attributed to bound water, which is thought to be one of countercations. It should be noted that no signals from the other sites appear at this region. A signal at ∼5 ppm is assigned to glycerol protons ($RCH_2O$), which was seen for each spectra.

From Figure 3 b,c, one can realize that a signal which was not seen in the spectrum of the DPPA sample appeared at ∼9 ppm. The signal can be assigned to the phosphate proton which has a different electronic structure from that of the signal at ∼10 ppm. This indicates that the electronic structure of phosphate head-group in DPPA is changed by the complexation with the acidic polypeptides. Furthermore, it is found that the signal at ∼6 ppm appeared roughly twice the intensity as that observed in DPPA. For DPPA/pARG, the extra signal at ∼4 ppm was assigned to the NH protons not participating in hydrogen-bonding. This can be attributed to the NH protons of the side chain of the acidic polypeptides. By performing $^{31}$P−$^{1}$H HETCOR measurements, we were able to detect the intermolecular interaction of the phosphate/amine ion complexes in DPPA/pLYS and DPPA/pARG. Furthermore, it can be said that $^{31}$P−$^{1}$H HETCOR NMR spectroscopy would be applicable to the detection of intermolecular interactions found in several phosphate/amine complexes.

**$^{31}$P Chemical Shift Tensors of DPPA/pLYS and DPPA/pARG Polyion Complexes.** In our previous study, we performed $^{31}$P CPMAS measurements of DPPA/pLYS and DPPA/pARG complexes at room-temperature condition and determined principal components of the $^{31}$P chemical shielding tensors (CSTs) from SSB intensities. Table 1 summarizes the results of principal components for the $^{31}$P CSTs. While the chemical

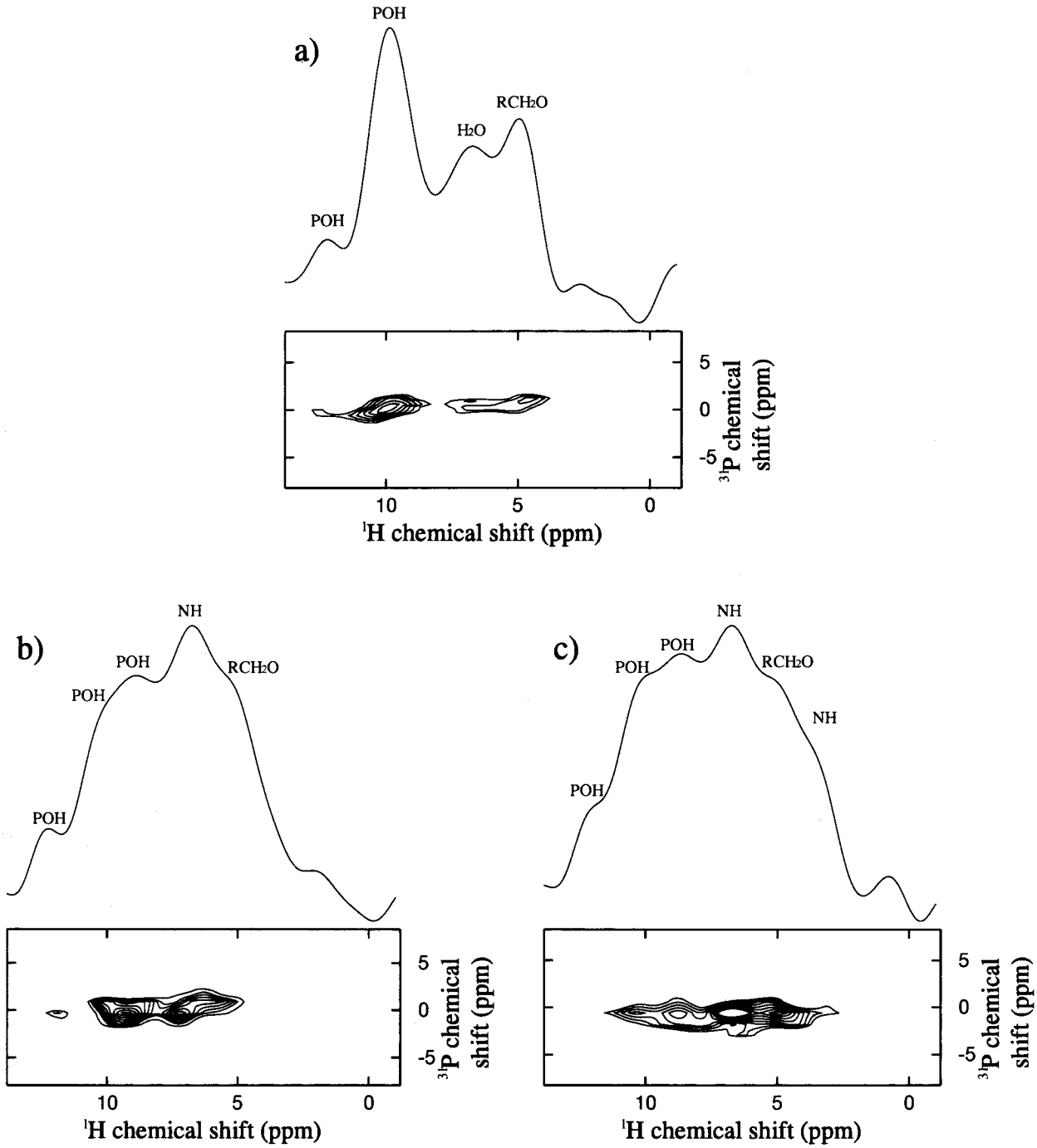


**Figure 3.** $^{31}P-^{1}H$ HETCOR spectra for lyophilized powder of (a) DPPA, (b) DPPA/pLYS, and (c) DPPA/pARG complexes.

**TABLE 1: Experimental Principal Components of $^{31}P$ Chemical Shift Tensors for DPPA, DPPA/pLYS, DPPA/PARG[a]**

| compound | $\delta_{iso}$ | $\delta_{11}$ | $\delta_{22}$ | $\delta_{33}$ | $\Delta\delta$ |
|---|---|---|---|---|---|
| DPPA | 0.0 | 66.7 | 12.6 | −79.3 | 119.0 |
| pLYS/DPPA | −1.2 | 61.9 | −1.2 | −64.3 | 94.7 |
| pARG/DPPA | −1.0 | 62.4 | 6.1 | −71.5 | 105.8 |

[a] The unit is parts per million (ppm). The isotropic chemical shielding of DPPA is defined as 0 ppm with respect to the experimental values.

shift anisotropy(CSA), which can be defined as the following:

$$\Delta\delta = \delta_{33} - \frac{1}{2}(\delta_{11} + \delta_{22}) \quad (1)$$

for the lyophilized sample of pure DPPA is as large as 119.0 ppm, the CSAs for the DPPA/pLYS and DPPA/pARG complexes are reduced to 94.7 and 105.8 ppm, respectively. The decrease of CSA value is more pronounced for the DPPA/pLYS complex. Additionally, the isotropic chemical shift values for DPPA/pLYS and DPPA/pARG appear in the upper field of 1.2 and 1.0 ppm, respectively, than the shift for DPPA. It is worth mentioning that for both complexes, the values of $\delta_{iso}$, $\delta_{11}$, and $\delta_{22}$ are decreased, and on the other hand, $\delta_{33}$ increased. This tendency for both the complexes might be regulated by a common mechanism.

One of such mechanisms for the $^{31}P$ chemical shielding tensor in phosphate compounds has been investigated by Turner et al.[26] They have demonstrated that a CSA value, $\Delta\delta$, of $^{31}P$ in phosphate compounds is correlated with the average deviation of O−P−O bond angles in a phosphate and the equation of

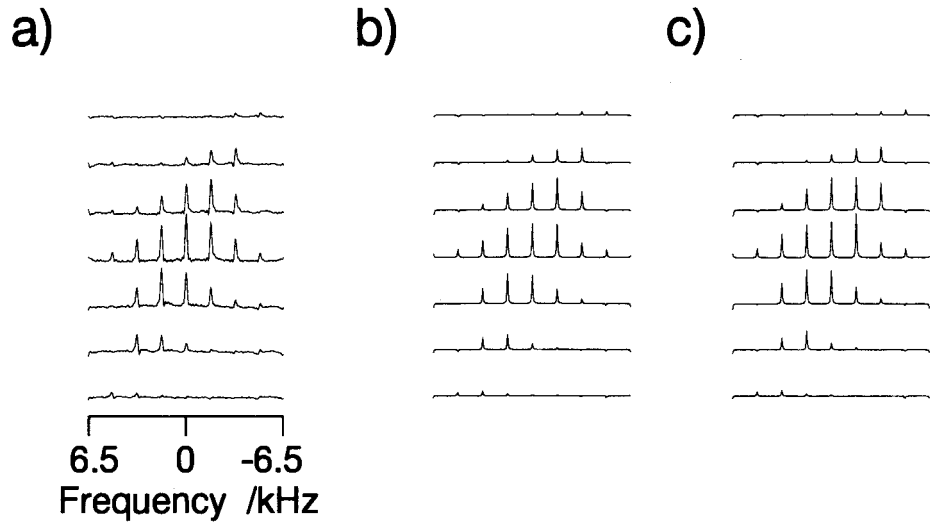


**Figure 4.** Spectra of separated local field measurements with SSB enhancement for (a) $MGD/H_2PO_4$ and (b) the spectrum simulation assuming a $SI_2$ spin system with best fitted parameters: $D_{P-H_1} = D_{P-H_2} = 4.0$ kHz, $(\psi, \chi, \xi) = (25°, 85°, 55°)$. (c) is the spectrum simulation with assuming an ideal tetraheral $H_2PO_4$ ($D_{P-H_1} = D_{P-H_2} = 4.0$ kHz, $(\psi, \chi, \xi) = (90°, 90°, 55°)$.

relationship is empirically

$$\Delta\delta(\text{ppm}) = 30.90\frac{\sum^{n}|109.5 - \theta\text{O}-\text{P}-\text{O(deg)}|}{n} - 1.22 \quad (2)$$

In consideration of the discussion by Turner et al., the complex formation of DPPA with the polypeptides might cause alteration in O−P−O angles in the phosphate group. The detailed analysis concerning this will be described in the section of chemical shielding calculation.

**Relative Orientation of $^{31}$P CST in Methylguanidinium Dihydrogenorthophosphate.** It is of great importance for researchers to obtain the information about orientation of CST as well as principal values of it. So far, no information about the orientation of the chemical shielding tensor with respect to the molecular fixed frame of the phosphate/amine complex has been obtained from powder spectra. For the quantitative interpretation of phospholipid bilayer spectra, one therefore makes the assumption that the orientation of the shielding tensor is the same as that observed in the single crystal of phosphoethanol amine.[27,28]

One of candidates for determination of orientation of CST from a powder sample is separated local field (SLF) measurements[29] with MAS. Since a typical heteronuclear $^{31}$P−$^{1}$H dipolar coupling for phosphate compounds would unfortunately be as small as 1 kHz, it is difficult, however, to perform the determination of orientation of CST from the observation of dipolar spinning sideband (SSB) patterns at a moderate MAS condition of 3−4 kHz. We thus attempted the enhancement of SSB intensities by using the enhanced spin−echo SLF described by Kolbert et al.[21] Methylguaniginium dihydrogenphosphate-($MGD/H_2PO_4$) is thought of as being one of model compounds displaying the local structure of the pARG/DPPA complex. We tried to determine the orientation of the $^{31}$P CST with respect to a molecular fixed frame. Figure 4 shows the SSB enhanced spin−echo SLF spectra for $MGD/H_2PO_4$. Before performing the determination of the orientation of CST, we performed Herzfeld−Berger analysis of the CPMAS spectrum, in order to obtain principal components of CST. The principal components of the chemical shift tensor were determined as $(\delta_{11}, \delta_{22}, \delta_{33}) = (66.95, -2.24, -64.71$ ppm). On the basis of the information about the CST components, the orientation of the CST was determined by comparing the experimental result of the enhanced spin−echo SLF with spectral simulation with assuming the three-spin system, $SI_2$. Here, it should be noted that the spectral fitting was carried out without taking into account the main peak of the dipolar spectra for isotropic chemical shift signal. The orientations of $^{31}$P CST with respect to the dipolar fixed frames for P−$H_1$ and P−$H_2$ are determined as $(\psi, \chi, \xi) = (25°, 85°, 55°)$, where the set of angles $(\psi, \chi, \xi)$ are defined as shown in Figure 5. Although orientation of two proton atoms directly bound to the phosphate group is defined by two sets of polar angles, we used an alternative definition by Munowitz et al.[29] because of convenience (Figure 5), where the orientation is defined by three variables of $(\psi, \chi, \xi)$ and one constant angle of $\angle H_1-P-H_2$ ($2\zeta = 112°$, typically). The magnitudes of the dipolar couplings for P−$H_1$ and P−$H_2$ were assumed to be the same, and the scaling factor of $D_{P-H}$ by WHH-4 was assumed to be the same as the theoretically predicted value, 0.565. The $D_{P-H}$ value was determined as 4.0 kHz (corresponding to $R_{P-H} \sim 2.4$ Å). Figure 6 shows the contour maps of the sum of RMSD of simulated sideband intensities with all possible sets of $(\psi, \chi, \xi)$ from the experimental sideband intensities.

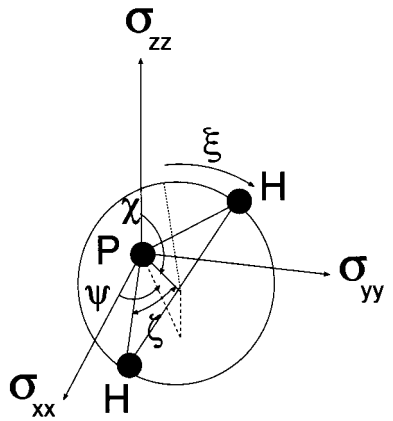


**Figure 5.** Schematical representation of the angles, $(\psi, \chi, \xi)$, which define the relative orientation of the bisector vector of the H−P−H angle with respect to the principal axis system for $^{31}$P chemical shift tensor. $2\zeta$ is defined as a H−P−H angle.

The orientation of the $^{31}$P CST for the powder sample of **IV** is roughly consistent with the previous results for the single crystals of phosphates.[27,28] However, the orientation determined here shows slight excursion from the typical orentation for the

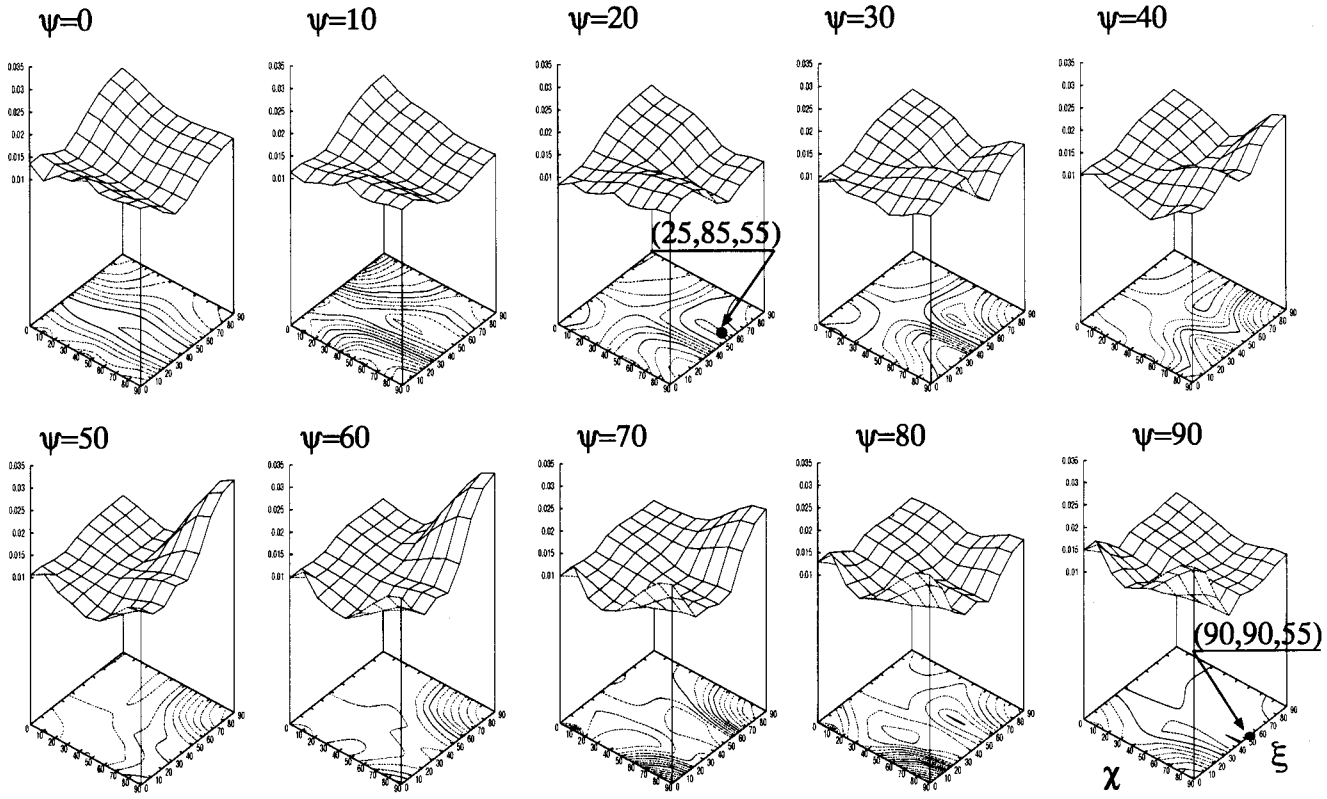


**Figure 6.** Contour maps of the sum of RMSD of simulated sideband intensities with all possible sets of ($\psi$, $\chi$, $\xi$), from the experimental sideband intensities.

ideal tetrahedral $PO_4$ group shown by Kohler et al.[27,28] Figure 4c is the simulated spin−echo SLF spectra with the ideal tetrahedron [($\psi$, $\chi$, $\xi$) = (90°, 90°, 55°)]. The slight excursion was also found in our ab initio GIAO chemical shielding calculation (Table 4, vide infra). The slight excursion might be attributed to the difference in the number of protonation of phosphate. To clearify this, one needs to make further spin−echo SLF measurements for several phosphate compounds.

**Chemical Shielding Calculation.** First, we performed ab initio GIAO chemical shielding calculations for the model molecules **I** and **II** in order to investigate whether one can explain the behaviors of the $^{31}$P experimental chemical shift tensor of the phosphate by altering the bond angle $O^{(3)}-P-O^{(4)}$ which could be expected in association with the complexation.

Figure 7 shows the results of $^{31}$P chemical shielding calculations for the model compounds **I** and **II**. Each points were calculated by using 6-31G(d,p) optimized structures with altering the $\angle O^{(3)}-P-O^{(4)}$ over the range from 88° to 115°. All the shielding calculations were carried out by using the 6-31G(d,p) basis sets. Regardless of the existense of the methyl ester, the $\sigma_{iso}$, $\sigma_{11}$, and $\sigma_{33}$ were monotonically decreased in accordance with decrease of $\angle O^{(3)}-P-O^{(4)}$. Only $\sigma_{22}$ was changed to the opposite direction. The tendency of the theoretical chemical shielding tensor is apparently different from that of the experimental results, where the $\sigma_{iso}$, $\sigma_{11}$, and $\sigma_{22}$ were shifted to the same direction, i.e., toward larger shielding. Therefore, the decrease of $\angle O^{(3)}-P-O^{(4)}$ caused by the DPPA/polypeptide complexation is less plausibly explained behavior of the observed chemical shift tensor.

Next, we examine the mechanism of how the phosphate/amine complexation would affect the $^{31}$P chemical shielding tensor of the phosphate. Table 2 shows the theoretical results for the model compounds, **III** and **IV**. $^{31}$P chemical shielding

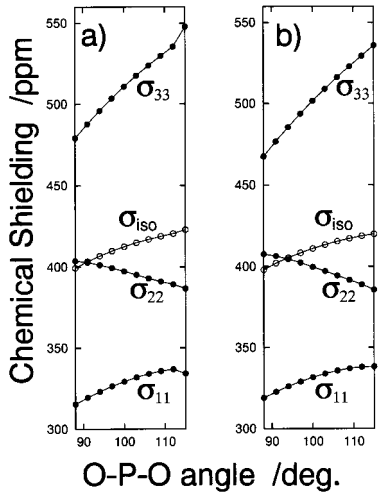


**Figure 7.** Dependence of $^{31}$P chemical shielding tensors for (a) model **I** and (b) **II** on the angle $O^{(3)}-P-O^{(4)}$.

were calculated with alteration of the intermolecular distance (**r**) between the phosphorus atom and the nitrogen atom in methylammonium or the carbon atom in guanidine. The definition of distance **r** is also drawn in Figure 8. The angle $\angle O^{(3)}-P-O^{(4)}$ was fixed at 112° and all the other geometrical parameters were optimized by using the 6-31G(d,p) basis sets. The shielding calculations were carried out by using the 6-31G(d,p) and 6-31++G(d,p) basis sets. For the model **IV** (corresponding to a model for the pARG/DPPA complex), the distances, $R^1_{OH}$ and $R^2_{OH}$ keep approximately the same as each other with respect to the alteration of **r**. On the other hand, as for the model **III** (corresponding to a model for the pLYS/DPPA complex), $R^1_{OH}$ and $R^2_{OH}$ are distinguishable for the longer value of **r** (> 3.7 Å) and a P−O···H−C type hydrogen bond can be seen as well as the P−O···H−N type at the region of **r**

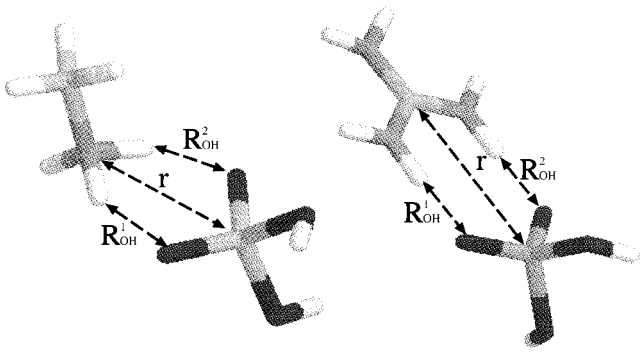


**Figure 8.** Definition of intermolecular distance (**r**) for model (a) **III** and (b) **IV**.

**TABLE 2: Variation of Principal Components of the Calculated $^{31}$P Chemical Shielding Tensors with Respect to Intermolecular Distance (r)**

| **r** [Å] | $R^1_{OH}$ [Å] | $R^2_{OH}$ [Å] | E(RHF) [au] | $\sigma_{iso}$ | $\sigma_{11}$ | $\sigma_{22}$ | $\sigma_{33}$ |
|---|---|---|---|---|---|---|---|
| $H_2PO_4^-$(GIAO-CHF/6-31G**//HF/6-31G**) | | | | | | | |
| | | | −641.478 | 420.4 | 336.8 | 389.2 | 535.4 |
| pLYS/DPPA Model (GIAO-CHF/6-31G**//HF/6-31G**) | | | | | | | |
| 3.90 | 3.50 | 2.28 | −737.240 | 419.0 | 344.1 | 406.9 | 506.2 |
| 3.70 | 3.10 | 2.08 | −737.249 | 419.1 | 346.1 | 406.6 | 504.7 |
| 3.50 | 2.04 | 2.03 | −737.259 | 419.1 | 351.8 | 406.0 | 499.5 |
| 3.30 | 1.84 | 1.84 | −737.268 | 419.9 | 358.2 | 406.9 | 494.7 |
| 3.10 | 1.65 | 1.65 | −737.270 | 421.1 | 365.2 | 407.5 | 490.6 |
| 2.90 | 1.48 | 1.47 | −737.261 | 422.4 | 372.5 | 408.9 | 485.7 |
| 2.70 | 1.37 | 1.34 | −737.229 | 423.7 | 377.6 | 411.1 | 482.4 |
| pARG/DPPA Model (GIAO-CHF/6-31G**//HF/6-31G**) | | | | | | | |
| 4.90 | 2.36 | 2.37 | −846.179 | 419.4 | 344.1 | 393.1 | 521.1 |
| 4.70 | 2.15 | 2.17 | −846.189 | 420.2 | 348.8 | 394.0 | 517.7 |
| 4.50 | 1.96 | 1.96 | −846.199 | 421.4 | 354.7 | 395.4 | 514.0 |
| 4.30 | 1.77 | 1.77 | −846.207 | 423.2 | 362.0 | 397.6 | 510.0 |
| 4.10 | 1.59 | 1.59 | −846.210 | 425.7 | 370.4 | 400.2 | 506.3 |
| 3.90 | 1.53 | 1.52 | −846.206 | 425.0 | 367.7 | 401.9 | 505.4 |
| 3.70 | 1.51 | 1.51 | −846.196 | 423.7 | 363.6 | 402.7 | 504.8 |
| $H_2PO_4^-$(GIAO-CHF/6-311++G**//HF/6-31G**) | | | | | | | |
| | | | −641.598 | 353.9 | 264.6 | 315.0 | 482.1 |
| pLYS/DPPA Model (GIAO-CHF/6-311++G**//HF/6-31G**) | | | | | | | |
| 3.90 | 3.50 | 2.28 | −737.376 | 354.7 | 274.0 | 340.3 | 449.8 |
| 3.70 | 3.10 | 2.08 | −737.384 | 354.8 | 276.0 | 339.8 | 448.7 |
| 3.50 | 2.04 | 2.03 | −737.394 | 355.4 | 283.4 | 339.9 | 443.0 |
| 3.30 | 1.84 | 1.84 | −737.401 | 357.0 | 291.3 | 341.2 | 438.6 |
| 3.10 | 1.65 | 1.65 | −737.402 | 359.4 | 301.2 | 342.2 | 434.9 |
| 2.90 | 1.48 | 1.47 | −737.391 | 361.9 | 311.4 | 344.2 | 430.2 |
| 2.70 | 1.37 | 1.34 | −737.357 | 364.1 | 318.4 | 346.9 | 427.1 |
| pARG/DPPA Model (GIAO-CHF/6-311++G**//HF/6-31G**) | | | | | | | |
| 4.90 | 2.36 | 2.37 | −846.342 | 354.5 | 273.5 | 322.5 | 467.5 |
| 4.70 | 2.15 | 2.17 | −846.352 | 355.0 | 276.7 | 323.9 | 464.3 |
| 4.50 | 1.96 | 1.96 | −846.361 | 356.0 | 281.5 | 325.7 | 461.0 |
| 4.30 | 1.77 | 1.77 | −846.369 | 358.0 | 288.4 | 328.3 | 457.4 |
| 4.10 | 1.59 | 1.59 | −846.371 | 361.0 | 297.5 | 331.5 | 454.2 |
| 3.90 | 1.53 | 1.52 | −846.366 | 360.4 | 296.8 | 332.1 | 452.3 |
| 3.70 | 1.51 | 1.51 | −846.355 | 359.6 | 295.0 | 332.5 | 451.2 |

(≥ 3.7 Å of which situation is depicted in Figure 9. Although it is unclear about whether the P−O···H−C type hydrogen bond exist in the pLYS/DPPA complex, this type of hydrogen bonding might be possible, since the side chain of pLYS is thought to be flexible to the rotational isomerization.

Regardless of basis sets used in this article, it appeared that there exists only single energetic minimum for both compounds along the reaction coordinate of **r**. It is found that the tendency of the experimental results are reproduced by the current ab initio GIAO chemical shielding calculation by taking into account the explicit complexation. This means that the effect of the phosphate/amine complexation on $^{31}$P chemical shielding

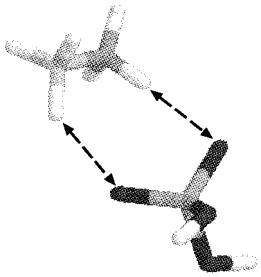

**Figure 9.** Drawing of P−O···H−C type hydrogen bonding found in the current MO calculation.

**TABLE 3. 6-31++G(d,p) GIAO $^{31}$P Chemical Shielding Tensors Calculated with 6-31G(d,p) Fully Optimized Geometry**

| compound | $\sigma_{iso}$ | $\sigma_{11}$ | $\sigma_{22}$ | $\sigma_{33}$ |
|---|---|---|---|---|
| pLYS/DPPA model | 358.8 | 291.4 | 338.9 | 446.1 |
| pARG/DPPA model | 360.5 | 290.8 | 332.5 | 458.2 |

**TABLE 4: Orientation of 6-311++G(d,p) ab Initio GIAO $^{31}$P Chemical Shielding Tensor with Respect to the Molecular Fixed Frame, for $H_2PO_4$, Mam/$H_2PO_4$, and GD/$H_2PO_4$**

| compound | $\psi$ | $\chi$ | $\xi$ |
|---|---|---|---|
| $H_2PO_4$ | 63 | 61 | 51 |
| MAM/$H_2PO_4$ | 89 | 78 | 78 |
| GD/$H_2PO_4$ | 85 | 63 | 88 |

tensor is more plausible explained by the observed CST behavior than by the effect of the alteration of the $O^{(3)}-P-O^{(4)}$ angle.

Finally, in order to compare the results of the pLYS/DPPA and pARG/DPPA complexes, the constraint of $\angle O^{(3)}-P-O^{(4)}$ was thus released and the 6-31++G(d,p) shielding calculations were performed with using the 6-31G(d,p) fully optimized geometrical parameters (Table 3). From Table 3, it can be said that the $\sigma_{11}$ and $\sigma_{22}$ values are larger for pLYS/DPPA than those for pARG/DPPA and the $\sigma_{33}$ value is smaller for pLYS/DPPA than that for pARG/DPPA. Furthermore, the differences in $\sigma_{22}$ between pLYS/DPPA and pARG/DPPA and also in $\sigma_{33}$ ($\Delta\sigma_{22}$ = 6.4 ppm and $\Delta\sigma_{33}$ = −12.1 ppm) are much larger than the difference in $\Delta\sigma_{11}$ (0.6 ppm). These tendencies can be seen in the observed results as well, and the current theoretical results quantitatively reproduce the experimental ones ([$\Delta\delta_{11}$, $\Delta\delta_{22}$, $\Delta\delta_{33}$] = [0.5, 7.3, −7.2 ppm]). As far as the orientation of the CSTs are concerned, although it has been believed that orientation of principal axis system of $^{31}$P chemical shielding tensor is insensitive to molecular species of phosphates, the slight deviation of the orientation of the observed $^{31}$P CST for MGD/$H_2PO_4$ from the well-known typical orientation of a tetrahedral $PO_4$ group was also seen in the 6-311++G(d,p) GIAO calculated orientation (Table 4). Additionally, the orientation for MAM/$H_2PO_4$ is slightly different from that for GD/$H_2PO_4$ as well as from that for $H_2PO_4$. One needs to perform further experiments and calculations of $^{31}$P CST for several phosphate compounds, in order to address systematic discussion.

## V. Conclusions

We were able to detect the intermolecular interactions in lyophilized powders of the pLYS/DPPA and pARG/DPPA complexes by the solid-state $^1$H−$^{31}$P heteronuclear correlation NMR spectroscopy. We succeeded in obtaining the complete information about $^{31}$P chemical shielding tensor for a phosphate group for a polycrystalline sample of MGD/$H_2PO_4$, by using both a conventional CPMAS and a SSB enhanced version of separated local field measurements. Based on the observed CST

and the ab initio GIAO chemical shielding calculation, the behaviors of $^{31}P$ chemical shielding tensor for the phosphate group in the two polyion complexes were reasonably explained by the changes in electronic structure of the phosphate group induced by the complexation rather than by decrease of O−P−O angles which was previously deduced in several phosphate compounds.

## References and Notes

(1) Pascal, S. M.; Singer, A. U.; Gish, G.; Yamazaki, T.; Shoelson, S. E.; Pawson, T.; Kay, L. E.; Forman-Kay, J. D. *Cell* **1994**, *77*, 461. Yamazaki, T.; Pascal, S. M.; Singer, A. U.; Forman-Kay, J. D.; Kay, L. E. *J. Am. Chem. Soc.* **1995**, *117*, 3556.

(2) Wu, C. *J. Biol. Chem.* **1997**, *272*, 28171.

(3) Lagier, C. M.; Zuriaga, M.; Monti, G.; Olivieri, A. *J. Phys. Chem. Solids* **1996**, *57*, 1183.

(4) Sandermann, H.; Mcintyre, J. O.; Fleischer, S. *J. Biol. Chem.* **1986**, *261*, 6201.

(5) Nishizuka, Y. *Nature* **1984**, *308*, 693.

(6) Bell, R. M. *Cell* **1986**, *45*, 631.

(7) Takahashi, H. et al. Personal communication.

(8) Takahashi, H.; Yasue, T.; Ohki, K.; Hatta, I. *Mol. Membr. Biol.* **1996**, *13*, 233.

(9) Takahashi, H.; Matuoka, S.; Kato, S.; Ohki, K.; Hatta, I. *Biochim. Biophys. Acta* **1991**, *1069*, 229.

(10) Saito, H.; Ando, I. *Annu. Rep. NMR Spectrosc.* **1989**, *21*, 209.

(11) Kurosu, H.; Ando, S.; Yoshimizu, H.; Ando, I. *Annu, Rep. NMR Spectrosc.* **1994**, *28*, 189.

(12) Asakawa, N.; Kameda, T.; Kuroki, S.; Kurosu, H.; Ando, S.; Ando, I.; Shoji, A. *Annu. Rep. NMR. Spectrosc.* **1998**, *35*, 55.

(13) Sato, D.; Asakawa, N.; Sakurai, M.; Inoue, Y. *J. Phys. Chem.* **1998**, *B102*, 3073.

(14) Pines, A.; Gibby, M. G.; Waugh, J. S. *J. Chem. Phys.* **1973**, *59*, 569.

(15) Schaefer, J.; Stejskal, E. O. *J. Am. Chem. Soc.* **1975**, *98*, 1031.

(16) Stejskal, E. O.; Schaefer, J.; Waugh, J. S. *J. Magn. Reson.* **1977**, *28*, 105.

(17) Cotton, F. A.; Hazen, E. E., Jr.; Day, V. W.; Larsen, S.; Norman, J. G., Jr.; Wong, S. T. K. *J. Am. Chem. Soc.* **1973**, *95*, 2367. Cotton, F. A.; Day, V. W.; Hazen, E. E., Jr.; Larsen, S. *J. Am. Chem. Soc.* **1973**, *95*, 4834. Cotton, F. A.; Day, V. W.; Hazen, E. E., Jr.; Larsen, S., Wong, S. T. K. *J. Am. Chem. Soc.* **1974**, *96*, 4471.

(18) Fenzke, D.; Maess, B.; Pfeifer, H. *J. Magn. Reson.* **1990**, *88*, 172.

(19) Herzfeld, J.; Berger, A. E. *J. Chem. Phys.* **1980**, *73*, 6021.

(20) Burum, D. P.; Bielecki, A. *J. Magn. Reson.* **1991**, *94*, 645.

(21) Kolbert, A. C.; Raleigh, D. P.; Levitt, M. H.; Griffin, R. G. *J. Chem. Phys.* **1989**, *90*, 679.

(22) Waugh, J. S.; Huber, L. M.; Haeberlen, U. *Phys. Rev. Lett.* **1968**, *20*, 180. Mehring, M. *Z. Naturforsh.* **1972**, *27a*, 1634. Mehring, M. *Z. Naturforsh.* **1973**, *A28*, 804. Mehring, M. *Rev. Sci. Instrum.* **1973**, *44*, 64.

(23) Liu, H.; Glaser, S. J.; Drobny, G. P. *J. Chem. Phys.* **1990**, *93*, 7543.

(24) Gerstein, B. C. *Philos. Trans. R. Soc. London* **1981**, *A299*, 521.

(25) Santos, R. A.; Wind, R. A.; Bronnimann, C. E. *J. Magn. Reson.* **1994**, *B105*, 183.

(26) Turner, G. L.; Smith, K. A.; Kirkpatrick, R. J.; Oldfield, E. *J. Magn. Reson.* **1986**, *70*, 408.

(27) Kohler, S. J.; Klein, M. P. *Biochemistry* **1976**, *15*, 967.

(28) Kohler, S. J.; Klein, M. P. *Biochemistry* **1977**, *16*, 519.

(29) Hester, R. K.; Ackerman, J. L.; Neff, B. L.; Waugh, J. S. *Phys. Rev. Lett.* **1976**, *36*, 1082. Munowitz, M. G.; Griffin, R. G. *J. Chem. Phys.* **1982**, *76*, 2848. Munowitz, M. G.; Griffin, R. G. *J. Chem. Phys.* **1983**, *78*, 613. Munowitz, M. G.; Huang, T.-H.; Griffin, R. G. *J. Chem. Phys.* **1987**, *86*, 4362. Ramamoorthy, A.; Wu, C. H.; Opella, S. J. *J. Magn. Reson.* **1995**, *B107*, 88. Hong, M.; Schmidt-Rohr, K. *J. Magn. Reson.* **1995**, *B109*, 284.